

Tumor suppressor microRNA-204-5p regulates growth, metastasis, and immune microenvironment remodeling in breast cancer.

Bok Sil Hong¹, Han Suk Ryu², Namshin Kim^{3,4}, Jisun Kim^{1,8}, Eunshin Lee^{1,8}, Hyunhye Moon¹, Kyoung Hyoun Kim^{3,4}, Min-Sun Jin⁵, Nam Hoon Kwon⁶, Sunghoon Kim^{6,7}, Donghyun Kim⁸, Doo Hyun Chung⁸, Kyeonghun Jeong⁹, Kwangsoo Kim⁹, Ki Yoon Kim¹⁰, Han-Byoel Lee¹¹, Wonshik Han^{11,12}, Jihui Yun¹², Jong-Il Kim¹², Dong-Young Noh^{11,12}, Hyeong-Gon Moon^{1,11,12}

¹Center for Medical Innovation, Biomedical Research Institute, Seoul National University Hospital, Seoul. ²Department of Pathology, Seoul National University Hospital, Seoul. ³Personalized Genomic Medicine Research Center, Division of Strategic Research Groups, Korea Research Institute of Bioscience and Biotechnology, Daejeon. ⁴Department of Functional Genomics, Korea University of Science and Technology, Daejeon. ⁵Bucheon St. Mary's Hospital, College of Medicine, The Catholic University of Korea, Bucheon. ⁶Medicinal Bioconvergence Research Center, Seoul National University, Suwon. ⁷Department of Molecular Medicine and Biopharmaceutical Sciences, Graduate School of Convergence Science and Technology, Seoul National University, Suwon. ⁸Department of Pathology, Seoul National University School of Medicine, Seoul, South Korea. ⁹Division of Clinical Bioinformatics, Biomedical Research Institute, Seoul National University Hospital. ¹⁰Department of Neurology, Seoul National University College of Medicine, Seoul, South Korea. ¹¹Department of Surgery, Seoul National University College of Medicine, Seoul, South Korea. ¹²Genomic Medicine Institute, Seoul National University Medical Research Center, Seoul, South Korea.

Running Title: Tumor suppressive role of miR-204-5p in breast cancer

Corresponding Author: Hyeong-Gon Moon, Seoul National University College of Medicine, 103 Daehak-ro, Jongno-gu, Seoul, 03080, South Korea. Phone: 82-2-2072-2634; Fax: 82-2-766-3975; E-mail: moonhg74@snu.ac.kr

Disclosure of Potential Conflicts of Interest: No potential conflicts of interest were disclosed.

Abstract

Various microRNAs (miRNAs) play critical roles in the development and progression of solid tumors. In this study, we describe the role of miR-204-5p in limiting growth and progression of breast cancer. In breast cancer tissues, miR-204-5p was significantly downregulated compared to normal breast tissues, and its expression levels were associated with increased survival outcome in breast cancer patients. Overexpression of miR-204-5p inhibited viability, proliferation, and migration capacity in human and murine breast cancer cells. Additionally, miR-204-5p overexpression resulted in a significant alteration in metabolic properties of cancer cells and suppression of tumor growth and metastasis in mouse breast cancer models. The association between miR-204-5p expression and clinical outcomes of breast cancer patients showed a non-linear pattern that was reproduced in experimental assays of cancer cell behavior and metastatic capacities. Transcriptome and proteomic analysis revealed that various cancer-related pathways including PI3K/Akt and tumor immune interactions were significantly associated with miR-204-5p expression. PIK3CB, a major regulator of PI3K/Akt pathway, was a direct target for miR-204-5p, and the association between PIK3CB-related PI3K/Akt signaling and miR-204-5p was most evident in the basal subtype. The sensitivity of breast cancer cells to various anti-cancer drugs including PIK3CB inhibitors was significantly affected by miR-204-5p expression. Additionally, miR-204-5p regulated expression of key cytokines in tumor cells and reprogrammed the immune microenvironment by shifting myeloid and lymphocyte populations. These data demonstrate both cell-autonomous and non-cell-autonomous impacts of tumor suppressor miR-204-5p in breast cancer progression and metastasis.

Statement of significance

This study demonstrates that regulation of PI3K/Akt signaling by miR-204-5p suppresses tumor metastasis and immune cell reprogramming in breast cancer.

Introduction

MiRNAs are involved in various cellular and physiological processes such as cell proliferation and differentiation, and the aberrant expression of miRNAs are associated with progression and metastasis of various human tumors (1, 2). Genome-wide miRNAs expression studies of breast cancers and normal tissues demonstrated the existence of breast cancer-specific miRNA signatures (3) and subtype-related microRNA expression patterns (4, 5).

To identify and characterize the miRNAs involved in breast cancer progression, we performed small RNA sequencing of breast cancer tissues and adjacent normal tissues, and found a substantial number of differentially expressed miRNAs including miR-204-5p that was significantly downregulated in breast cancer tissues. Several studies have shown that miR-204-5p is frequently downregulated in various human tumor tissues compared with normal tissues, such as endometrial carcinoma, colorectal cancer, glioma, and thyroid carcinoma, and has been suggested to act as a tumor suppressor in most types of cancer (6-9). However, in breast cancer, the studies on the miR-204-5p expression shows conflicting results suggesting a possible dual regulatory roles (10). While some studies showed upregulation of miR-204-5p in breast cancer tissues and the pro-proliferative role of miR-204-5p in breast cancer cells *in vitro* (11, 12), other studies suggested that decreased expression of miR-204-5p caused by the frequent genomic loss in breast cancer was associated with worse clinical outcome (13, 14).

In this study, we tried to provide a comprehensive understanding on the importance of miR-204-5p in breast cancer, ranging from functional biology in regulating cell behavior and in reprogramming microenvironments to the clinical relevance of miR-204-5p and its downstream molecules in human breast cancer tissues. Additionally, we examined the possibility targeting the miR-204-5p-dependent signaling pathway and elucidate the dose-dependent, non-linear effects of miR-204-5p in breast cancer.

Materials and Methods

Clinical samples

The frozen tumor tissues were obtained from the IRB-approved breast cancer biospecimen repository at Seoul National University Hospital (SNUH IRB number: 1405-088-580). The collection of the clinical and pathologic data for tumors used for the small RNA sequencing in this study was additionally approved by the institutional IRB (IRB number: 1205-017-408). All procedures were done in accordance with the Declaration of Helsinki. For small RNA-seq, total RNA was extracted using TRIzol reagent (ThermoFisher), and then we prepared libraries using TruSeq Small RNA Library Prep Kit (Illumina, Part# 15004197) according to manufacturer's protocols. *In situ* hybridization was performed using double-digoxigenin labeled miRCURY LNA miRNA detection probe for miR-204-5p (Qiagen) in 7 paraffin-embedded tissues of breast cancer (IRB number: 1712-141-909) according to manufacturer's protocol. Formalin-fixed paraffin-embedded tissues of 439 patients of breast cancer were used to construct the tissue microarray (15). Slides were stained against PIK3CB and scored positive based on intensity and localization. The slides were reviewed by two pathologists (H. S.R. and M. S. J.).

Generation of miR-204-5p overexpressing cells

4T1 murine breast cancer cells and MDA-MB-231 human breast cancer cells (ATCC) were cultured in RPMI 1640 or DMEM supplemented with 10% FBS and antibiotics/antimycotic, respectively. Cells were periodically screened for mycoplasma contamination and MDA-MB-231 cell was authenticated by short tandem repeat (STR) profiling from Korean Cell Line Bank (Seoul, South Korea). To generate miR-204-5p overexpressing cells, control or overexpression plasmids for miR-204-5p (Genolution Pharmaceuticals, Seoul, Korea) were transfected to cells using Lipofectamine 3000 (Invitrogen) according to the manufacturer's instruction and stable clones were selected using Zeocin.

TaqMan miRNA assay and RT-PCR

Stem-loop qRT-PCR assays using TaqMan miRNA probes (Applied Biosystems, assay ID:

000508) were performed to quantify the levels of the miR-204-5p. Reverse transcription reaction was prepared using TaqMan MicroRNA Reverse Transcription Kit (Applied Biosystems) and real-time qPCR was performed with TaqMan Universal PCR Master Mix in an Applied Biosystems 7500 System. For conventional qRT-PCR, the relative abundance of each transcript was assessed using SYBR Green PCR Master Mix and primer information is in Supplementary Table S1.

Proliferation, 3D cell culture, migration, and invasion assays

Cells were directly counted using a TC20 Automated Cell counter (Bio-Rad). Cell proliferation was measured with the CellTiter-Glo Luminescent Cell viability Assay (Promega). For 3D cell cultures, cells were seeded onto growth factor reduced Matrigel (BD Biosciences). Spheroid growth was monitored, and the dimensions were measured as described in (16). Spheroids were stained using LIVE/DEAD[®] Viability/Cytotoxicity Kit (Molecular Probe) for microscopic visualization.

Cell migration and invasion were assayed using a Transwell inserts (8 μ m pore, Falcon) with or without Matrigel. Cells were seeded in upper chambers and incubated for 24 hours. Migrated cells were fixed and stained with 0.1% Crystal Violet. For quantification, the stained cells were extracted with 10% acetic acid, and the absorbance was determined at 570 nm.

Animal experiments

Six-week-old female BALB/c and immune-deficient BALB/c Nude mice were purchased from Orient (Seoul, South Korea) and NOD/scid IL2Rg (null) (NSG) were purchased from the Jackson Laboratory. Cells ($1-2 \times 10^5$ /mouse) were orthotopically injected into mammary fat pad, and then tumor growth was monitored and volumes were calculated as $0.5 \times \text{length} \times \text{width}^2$. For experimental metastasis, cells were intravenously injected into the tail vein. After 2 weeks, Bouin's solution (Sigma)-fixed tissues were inspected for the metastatic nodules. All experiments were approved by the Institutional Animal Care and Use Committee in SNUH (IACUC approval no. 15-0284-C1A0).

Extracted tissues were analyzed for miR-204-5p expression and histologically evaluated with H&E staining. Immunohistochemical (IHC) protocol for Ki67 (Cell Signaling), PIK3CB, CCL20 and CD11b (Abcam) were performed at Pathology Core Facility in our institution. The IHC results were

quantified using the Immunoratio plugin available for the ImageJ software package (17).

RNA-Sequencing and bioinformatics

For RNA-seq of MDA-MB-231 xenograft tumor tissues generated in NSG mice, RNA-seq libraries were constructed using TruSeq Stranded mRNA Prep Kit (Illumina). Total RNA from 4T1 overexpressing miR-204-5p or control was purified and RNA-seq libraries were constructed using TruSeq RNA library preparation kit (Illumina). RNA-seq data analysis were conducted as detailed in Supplementary Data.

Extracellular acidification rate (ECAR) and oxygen consumption rate (OCR) measurements

Cells were plated in XF24 cell-culture microplates and the ECAR and OCR were assessed using an XF24 analyzer (Seahorse Bioscience). These data was normalized to the total protein contents, which were measured using a Bradford protein assay (Thermo Scientific).

Immunocytochemistry, Western blotting, and ELISA

To examine the morphological changes, cells were stained with CellTracker™ Green CMFDA (Molecular Probe), followed by incubation with CytoPainter Phalloidin-iFluor 488 Reagent (Abcam) after fixation. To check the PIK3CB levels, cells were stained with anti-*PIK3CB* (Abcam) and observed under confocal microscope.

For Western blotting, total proteins were separated by SDS-PAGE and then transferred to PVDF membrane. After blocking, the membrane was probed with specific antibodies against PIK3CB, phospho-Akt (Ser473) and Akt (Cell Signaling Technology), and β -actin (Santa Cruz) followed by the treatment of horseradish peroxidase conjugated secondary antibodies. Target proteins were detected using the Amersham Imager 600 (GE Healthcare) developed with enhanced chemiluminescent substrate (Thermo Scientific). For ELISA, Cell culture supernatants were collected, and the levels of CCL20 and VEGF-A was quantified using Qauantikine ELISA kit (R&D system).

Luciferase assay

To clone the 3'-UTR region of PIK3CB, oligos corresponding to a 66-bp or 67-bp fragment from the 3'-UTR of the murine *Pik3cb* and human PIK3CB were synthesized with XhoI at 5'-end and NotI at 3'-end. The target sequence was predicted by miRNA target prediction program, miRDB (<http://mirdb.org/>), listed in Fig. 4D. As a negative control, we also designed oligonucleotides containing a mutated miR-204-5p target site, by replacing the seed regions of the target site with T₍₇₎ (18). These annealed oligonucleotides were purchased from Bioneer Inc. (South Korea) and cloned into psiCHECK-2 vector (Promega). For luciferase activity assay, cells were co-transfected with negative control and miR-204-5p mimics along with psiCHECK-2 vector containing wild type or mutated 3'UTR of PIK3CB using Lipofectamine 3000. After 24 h of transfection, cells were reseeded in 96-well plates, and luciferase activities were measured with Dual-Glo Luciferase Assay system (Promega). Renilla luciferase activity was normalized to firefly luciferase activity.

RNA interference, overexpression, and inhibition of PIK3CB

To knockdown PIK3CB, cells were transfected with on-target plus non-targeting control siRNA and siRNA for human PIK3CB (5291) (Dharmacon) using Lipofectamine RNAi MAX reagent (Thermo Scientific). For overexpression of PIK3CB, pCMV hygro negative control vector or human PIK3CB containing vector were used (Sino Biological Inc). Cells were transfected with control or PIK3CB vector using Lipofectamine 3000. For PIK3CB inhibition, cells were treated with TGX-221 and GSK2636771 (Selleckchem) for indicated time.

Flow cytometry of immune cells from tumor tissue

The cells from 4T1-tumor tissue were isolated as previously described with some modifications (19). The anti-mouse antibodies (BioLegend) used for flow cytometry were as follows: CD45 (30-F11), TCR β ⁺ (H57-597), CD4 (RM4-5), CD8 (53-6.7), NK1.1 (PK136), Foxp3 (MF-14), CD11b (M1/70), F4/80 (BM8), CD11c (N418), CD206 (CD68C2), Gr-1 (RB6-8C5), Ly6G (1A8), Ly6C (HK1.4).

Statistical analysis

In general, most data represent the mean \pm S.D and are representative of 3 independent

experiments, except for 3D spheroid growth, *in vivo* tumor growth and pulmonary metastasis experiments. GraphPad Prism was used for generating graphs and heatmaps and performing statistical tests. *P* values were calculated from unpaired two-tailed Student's *t* tests, based on comparisons with the appropriate control samples tested at the same time, *, ** or *** indicates *P*<0.05, *P*<0.01, *P*<0.001 respectively. Kaplan-Meier survival curves with log-rank tests were evaluated to analyze the time to progression and survival. The χ^2 and Fisher exact test were used to analyze the association between PIK3CB and clinicopathologic variables.

Data Availability Statement

The small RNA-seq and RNA-seq data generated in the present study have been deposited in NCBI Gene Expression Omnibus with the accession number GSE109725. Additional information on the clinical characteristics of the involved patients are available by contacting the corresponding author.

Results

Decreased expression of miR-204-5p in human breast cancer and its relationship with patient's survival

First, we identified 106 differentially expressed miRNAs between breast cancer tissues and normal breast tissues by using RNA sequencing of tissues from 17 breast cancer patients (Fig. 1A; Supplementary Fig. S1A and S1B). Among these, miR-204-5p was the most significantly downregulated miRNA in all 17 breast cancer tissues (Fig. 1B; Supplementary Fig. S1C). The down-regulation of miR-204-5p in breast cancer was validated in an independent cohort of 32 breast cancer patients (Fig. 1C; Supplementary Fig. S1D). Next, we performed *in situ* hybridization against miR-204-5p to determine the tissue expression patterns using breast tissues from seven breast cancer patients. In five out of seven cases, normal mammary epithelial cells showed higher miR-204-5p expression when compared to adjacent breast cancer cells (Fig. 1D; Supplementary Fig. 1E). Interestingly, two cases showed topographic differences in miR-204-5p levels suggesting some tumors may have intra-tumoral heterogeneity in miR-204-5p expression. Also, the miR-204-5p down-regulation was seen in low grade *in situ* tumors suggesting the loss of miR-204-5p may occur during the early phase of premalignant transition.

To further validate the decreased expression of miR-204-5p in breast cancer, we analyzed the breast cancer (BRCA) miR-seq data from TCGA. When stratified by tumor stages and PAM50 subtypes, miR-204-5p expression was significantly decreased across all stages and subtypes (Supplementary Fig. S1F; Fig. 1E). The down-regulation of miR-204-5p in tumor tissues was also observed for most of the solid tumor types in TCGA datasets (Supplementary Fig. S1G). Human miR-204-5p transcript arise from the intronic area of transient receptor potential melastatin-3 (TRPM3) gene of which the mRNA expression level correlates the miR-204-5p level (Fig. 1F) (20). We identified two CpG loci in TRPM3 gene (cg20555507 and cg21251785) which are likely to influence the miR-204-5p expression (Fig. 1G). The cg20555507 locus was significantly hypermethylated in breast cancer tissues across various subtypes (Fig. 1H). The cg21251785 locus showed significantly higher degree of methylation that correlate the miR-204-5p expression only in basal subtype breast cancer (Fig. 1I; Supplementary Fig. S1H). We also examined the copy number alterations of miR-204-

5p-encoding region since 9p21.12 chromosomal region that encodes hsa-miR-204-5p is lost in up to 28% of breast cancers (14). A subset of TCGA cases showed copy number alterations at TRPM3 gene (Supplementary Fig. S1I and S1J), but even cases with TRPM3 copy number gain still showed down-regulation of miR-204-5p.

When the TCGA cases were classified into two groups based on their miR-204-5p levels, tumors with high miR-204-5p expression showed significantly better overall survival ($p=0.0045$, log-rank test; Fig. 1J). Interestingly, when patients were classified into quartiles, we found that the group of third quartiles whose tumors had intermediate miR-204-5p expression showed significantly better overall survival (hazard ratio [HR]=0.4870, 95% CI: 0.2420-0.9790, $p=0.041$; Fig. 1K; Supplementary Fig. S1K). In gene set enrichment analysis (GSEA), the third quartile group was enriched with pathways involved in immune cell modulation and cytokine interactions when compared to other quartiles (Fig. 1L; Supplementary Fig. S2A). In contrast, the fourth quartile group with highest miR-204-5p was enriched with Wnt/ β -catenin signaling and TNFA signaling when compared to the third quartile group (Supplementary Fig. S2B).

We also measured the miR-204-5p levels in paired tumor and metastasis samples obtained from two patient-derived xenograft models of triple negative breast cancer (TNBC) cases that developed spontaneous metastasis to liver and lung, respectively. MiR-204-5p levels did not show significant difference between primary tumor and metastatic tissues (Supplementary Fig. S2C). Additionally, we observed no significant difference between primary tumor and metastasis using seven TCGA cases where sequencing data were available for both primary tumor and metastasis (Supplementary Fig. S2D and S2E).

Taken together, these data indicate that miR-204-5p is down-regulated in human solid tumors including breast cancer and its down-regulation is mostly resulting from TRPM3 hypermethylation in tumor tissues. The level of miR-204-5p expression in tumor tissue showed non-monotonic association with clinical features. In breast cancer, tumors with intermediate miR-204-5p expression showed improved survival and were associated with molecular features of tumor-immune interactions. The down-regulation of miR-204-5p in breast cancer seem to occur in early phase of malignant transformation and was maintained during the process of metastasis.

MiR-204-5p suppresses tumor growth and metastasis, and reprograms metabolic pathways in breast cancer cells.

Based on the miRNA database (miRBase ver. 21), the sequences of the mature miR-204 from 10 different species are completely conserved from mammalian to fish (Supplementary Fig. S3A). To examine the role of miR-204-5p in breast cancer progression, we first established a MDA-MB-231 human TNBC cell line that stably overexpress miR-204-5p (Supplementary Fig. S3B and S3C). MiR-204-5p overexpression significantly reduced the growth rate (Fig. 2A) and the size of 3D-cultured tumor spheroids (Fig. 2B and C) by inducing G2/M arrest (Supplementary Fig. S3D). Additionally, the migratory activity of breast cancer cells was also decreased by miR-204-5p overexpression (Fig. 2D). Next, we investigated the effect of miR-204-5p on *in vivo* tumor growth by injection of control and miR-204-5p overexpressing cells into the mammary fat pads of NSG mice. Overexpression of miR-204-5p effectively suppressed the xenograft tumor growth (Fig. 2E), and reduced the number of Ki67+ cells (Fig. 2F). The MDA-MB-231 xenograft tumors from control cells often developed metastases to the lung and liver (Fig. 2G and H). However, the miR-204-5p overexpressing cells showed substantial reduction in the incidence of metastasis (Fig. 2G and H).

Transcriptome sequencing of the xenograft tumors showed that genes involved in Hippo signaling and TGF β signaling were most affected by miR-204-5p overexpression (Fig. 2I). The differentially expressed Hippo signaling genes included MYC, YAP1, TAZ (Supplementary Fig. S3E-S3G) which are known regulators of cell metabolism (21, 22). Additionally, GSEA using xenograft RNA seq data showed miR-204-5p expression levels affect metabolism-related pathways such as mTOR signaling or oxidative phosphorylation (Supplementary Fig. S3H). These findings led us to examine the metabolic characteristics associated with miR-204-5p. When we compared the metabolic phenotypes of control and miR-204-5p overexpressing MDA-MB-231, overexpression of miR-204-5p significantly reduced in oxygen consumption rates as well as extracellular acidification rates (Fig. 2J and 2K).

These results indicate that miR-204-5p inhibits tumor cell proliferation and migration *in vitro* and tumor growth and metastasis *in vivo*. Overexpression of miR-204-5p in breast cancer cell resulted in

perturbation in genes involved in cancer metabolism and significantly suppressed the metabolic activities of cancer cells.

MiR-204-5p has biphasic effects on the suppression of tumor growth and metastasis

As we previously observed that miR-204-5p showed biphasic role in breast cancer survival according to their expression levels from TCGA dataset, we hypothesized that miR-204-5p might also have similar effects on tumor growth and metastasis in mouse breast cancer model. To test this, we established stable 4T1 clones overexpressing different levels of miR-204-5p. The miR-204-5P overexpressing clones, C#1 to C#4, showed fold increase of 17.7 ± 1.2 , 150.3 ± 7.8 , 525.0 ± 62.1 , and 1419.0 ± 37.7 compared to control in terms of miR-204-5p expression (Fig. 3A). When injected into the mammary fatpads of syngeneic BALB/c mice, C#3 cells showed significant reduction in tumor growth and incidence of Ki67+ cells compared to control cells while the C#4 cells, which showed more than twofold higher miR-204-5p expression than C#3, showed no such effect (Fig. 3B-D). The different degrees of miR-204-5p in each clone were maintained in xenograft tumors (Fig. 3E). Furthermore, the tumor weight of C#4 xenograft tumor was positively correlated with the miR-204-5p expression (Fig. 3F).

We next examined the effect of miR-204-5p on tumor metastasis by introducing tumor cells *via* tail vein. After two weeks, control 4T1 cells showed extensive metastatic lesions in the lung, whereas C#3 almost completely suppressed the lung metastasis (Fig. 3G and H). Interestingly, C#2, which expressed moderate degree of miR-204-5p overexpression and failed to suppress orthotropic tumor growth, also inhibited the lung metastasis in similar degree with C#3. However, C#4, which had highest levels of miR-204-5p overexpression, did not show any suppressive effect on lung metastasis development.

In concordance with the *in vivo* results, C#3 had most distinct reduction in the rate of cell growth and the number of proliferating cells when compared to those of control cells *in vitro* (Fig. 3I; Supplementary Fig. S4A and S4B). Additionally, the C#2 and C#3 clones showed scattered cell morphology compared to control cells while C#4 showed restoration of cell adhesion ability (Fig. 3J). The *in vivo* and *in vitro* results showing the lack of tumor-suppressive effect of C#4 clone suggested

possible mesenchymal-epithelial transition (MET) in cells expressing excessive levels of miR-204-5p. Indeed, the mRNA and protein levels of E-cadherin were significantly upregulated in C#4 clone compared to other clones (Supplementary Fig. S4C; Fig. 3K). These observations, along with above analysis using TCGA dataset, suggest that miR-204-5p exerts dose-dependent biphasic effect on tumor growth and metastasis formation in breast cancer.

MiR-204-5p regulates PI3K/Akt pathways in breast cancer via targeting PIK3CB

To understand the molecular mechanism of the miR-204-5p's effect on cancer cells, we performed transcriptome profiling of miR-204-5p overexpressing C#2 and C#3 cells using RNA sequencing (Supplementary Fig. S5A). Pathway analysis using the differentially expressed genes again showed that miR-204-5p was involved in various cancer-related pathways, such as transcriptional misregulation in cancer, TNF signaling, focal adhesion, PI3K/Akt signaling, and tumor-immune interactions (Fig. 4A; Supplementary Fig. S5B and S5C). The expression levels of genes that are known to be involved in the various cancer-related pathways were further validated by RT-qPCR (Supplementary Fig. S5D and S5E).

Next, to gain insights on miR-204-5p-related proteomic changes in signaling pathways, we carried out an integrative analysis using TCGA datasets of miRNA-seq and RPPA (reverse phase protein microarray). Various cancer-related proteomic pathways were associated with miR-204-5p expression status including PI3K/Akt, TSC/mTOR, cell cycle, and apoptosis (Supplementary Fig. S6A and S6B). Importantly, there were significant inverse correlations between miR-204-5p expression and phosphorylation degree of Akt, mTOR, and other phosphoproteins in PI3K/Akt/mTOR signaling, particularly in basal subtype (Fig. 4B; Supplementary Fig. S6C). Additionally, we observed a significant negative relationship between the miR-204-5p expression and the PI3K/Akt signaling activity as measured by the PI3K/Akt signature score (Fig. 4C) (23). Based on our RNA sequencing data and TCGA proteomic data, we hypothesized that miR-204-5p might be a key regulator of PI3K/Akt signaling pathway, especially in basal subtype breast cancers.

To identify the potential target genes of miR-204-5p, we compared differentially expressed genes with miR-204-5p candidate target genes predicted by TargetScan and miRDB (Supplementary Fig.

S7A and S7B). Among the overlapping genes, we selected PIK3CB, a catalytic subunit of phosphatidylinositol-4,5-bisphosphate 3-kinase encoding p110 β , for further experiments as the PI3K/Akt signaling pathway was the major pathway influenced by the miR-204-5p expression. Using the luciferase reporter assay, we observed that PIK3CB is indeed a direct target of miR-204-5p (Fig. 4D and E, Supplementary Fig. S7C-F). Also, ectopic expression of miR-204-5p resulted in decreased expression levels of PI3KCB mRNA and protein, and affected the downstream Akt phosphorylation in breast cancer cells (Fig. 4F-H, and Supplementary Fig. S7G). Moreover, the immunohistochemical staining activities of PIK3CB from tumors that overexpress miR-204-5p were significantly lower than that of control tumors (Fig. 4I), and relatively weaker intensity of phospho-mTOR was observed in tumor tissues by miR-204-5p overexpression compared to control (Supplementary Fig. S7H). These results indicate that PIK3CB is a direct target of miR-204-5p that mediates miR-204-5p's effects on PI3K/Akt signaling activities.

To delineate the functional importance of PIK3CB in breast cancer cells, we silenced PIK3CB expression in MDA-MB-231 cells using siRNA against PIK3CB (Fig. 5A). siPIK3CB treatment resulted in downregulation of phospho-Akt (Fig. 5B), and inhibition of cell proliferation, 3D tumor growth, and migratory activity as seen in miR-204-5p overexpressing cells (Fig. 5C-E; Fig. 2A-D). In contrast, PIK3CB overexpression resulted in increased cell proliferation and cell migration in breast cancer cells (Fig. 5F-H). However, PIK3CB overexpression in miR-204-5p-overexpressing cells failed to induce such changes possibly due to the inhibitory effect of miR-204-5p on PIK3CB protein levels (Fig. 5F-H).

We further tested whether PIK3CB inhibition can show anti-tumor effects by using PIK3CB inhibitor, TGX-221 and GSK-2636771. Several breast cell lines (MCF10A, HCC70, MDA-MB-468) showed response to both PIK3CB inhibitors while MDA-MB-231 cells showed minimal responses (Supplementary Fig. 8A). However, ectopic expression of miR-204-5p in MDA-MB-231 cells resulted in an increased sensitivity to both PIK3CB inhibitors (Fig. 5I and J; Supplementary Fig. 8B). Since PI3K/Akt signaling pathway has been reported to be widely involved in chemotherapeutic resistance (24), we tested the response to various chemotherapeutic agents in miR-204-5p overexpressing cells. Breast cancer cells overexpressing miR-204-5p showed increase sensitivity to doxorubicin, taxanes,

and bortezomib when compared to control cells (Fig. 5K).

These data suggest that miR-204-5p is an important regulator in PI3K/Akt signaling via inhibiting PIK3CB. Overexpression of miR-204-5p confers increased sensitivity to PIK3CB inhibitors and to cytotoxic chemotherapeutic agents.

Clinical implications of miR-204-5p and its target gene, PIK3CB, in breast cancer

Next, we investigated the clinical significance of PIK3CB in breast cancer using human breast cancer tissues and TCGA breast cancer datasets. PIK3CB mRNA expression levels were significantly increased in breast cancer tissues compared to adjacent normal tissues (Fig. 6A -C). The PIK3CB mRNA levels were significantly correlated with miR-204-5p levels (Fig. 6D and E; Supplementary Fig. S9A). The negative relationship between PIK3CB and miR-204-5p was highly significant in the basal subtype (Supplementary Fig. S9B; Fig. 6F and G). In breast cancer cell lines, we observed strong PIK3CB expression mostly in cells with basal characteristics such as MDA-MB-157, MDA-MB-231, and Hs578T suggesting the potential activity of PIK3CB in basal breast cancer (Fig. 6H; Supplementary Fig. S9C).

We further analyzed the TCGA dataset for the possible association between PIK3CB expression and survival outcome. As expected, patients with higher expression of PIK3CB had worse 10-year overall survival compared with that of patients with lower PIK3CB expression (Fig. 6I, Supplementary Fig. S9D and S9E). Our TCGA dataset analysis indicate that, in human breast cancer, the PIK3CB expression is significantly correlated with miR-204-5p levels and is associated with differences in survival outcomes.

Since Kumar et al (25) have suggested the importance of the intracellular localization of PIK3CB, we evaluated the clinical importance of subcellular PIK3CB localization in a breast cancer tissue microarray (TMA) comprising samples from 438 patients. We categorized the PIK3CB staining results as negative (n=285), cytoplasmic PIK3CB (n=117), and nuclear PIK3CB (n=36) (Fig. 6J). The expression status of PIK3CB in breast cancer tissue was significantly associated with various important clinical parameters such as histologic grade, ER/PR status, and HER2 overexpression (Supplementary Table 2; Supplementary Fig. S9F). Often, the tumors showing cytoplasmic

expression of PIK3CB was more likely to carry poor prognostic factors such as higher histologic grade and ER negativity. However, PIK3CB was not an independent prognostic factor when adjusted for other factors (Supplementary Fig. S9G and Supplementary Table 3).

MiR-204-5p reprograms immune microenvironment in breast cancer

During the *in vivo* xenograft experiments, we noticed that the spleens of the mice harboring control MDA-MB-231 cells showed spleen enlargement. Interestingly, mice bearing miR-204-5p overexpressing tumors had significantly reduced spleen volumes and showed less alterations in splenic structures (Fig. 7A and 7B). As splenomegaly has been reported to be correlated with the amounts of myeloid cells (26), we stained the spleen with CD11b, a pan-myeloid marker, and observed a significant reduction of splenic CD11b+ myeloid cells in mice bearing the miR-204-5p overexpressing tumors (Fig. 7C).

In addition to the difference in size change and myeloid cell recruitment in spleens, our RNA seq data has also shown that pathways regulating tumor-immune interactions including cytokine-cytokine receptor interaction were significantly dysregulated in miR-204-5p-overexpressing human and mouse breast cancer cells (Fig. 4A). Several genes within the immune-related pathways including *Ccl20*, *Vegf-a/c*, *Pdfigb*, and *Csf1* showed significant association with the miR-204-5p expression status. (Supplementary Table 4). Furthermore, miR-204-5p expression was highly associated with immune pathways in TCGA dataset (Supplementary Fig. S2A). These findings led us to hypothesize that miR-204-5p may regulate the tumor-immune interactions within the tumor microenvironment. The downregulation of above cytokines in the cells overexpressing miR-204-5p were experimentally validated in both 4T1 and MDA-MB-231 cells (Fig. 7D-F), and the decreased expression of *Ccl20*, the most downregulated cytokine by miR-204-5p, was further verified in tumor tissues at protein levels (Fig. 7G and H). Moreover, the degree of CD11b+ myeloid cell infiltration was significantly reduced in tumors with miR-204-5p overexpressing breast cancer cells (Fig. 7G and H). Next, we extracted mouse RNA expression data from the MDA-MB-231 xenograft tumor RNA sequencing experiment by obtaining sequence reads aligned to the mouse genome. Mouse RNA expression data showed that miR-204-5p overexpression in human cancer cells resulted in significant alteration in the mouse

microenvironment cells. MiR-204-5p expression induced up-regulation of genes involved in the cytokine-cytokine receptor interaction along with other immune-related pathways in the microenvironment cells (Fig. 7I and Supplementary Fig. S10A and S10B)

To gain a more comprehensive understanding of the miR-204-5p-induced reprogramming of the immune microenvironment, we collected the allograft tumors overexpressing miR-204-5p in a 4T1 syngeneic mouse model and performed immune profiling using polychromatic flow cytometry. When compared to the control tumors, the miR-204-5p overexpressing tumors (C#3) showed substantial shifting in the composition of various immune cells in the tumor microenvironment (Fig. 7J; Supplementary Fig. S10C and S10D). There were significant reductions in MDSC (myeloid derived suppressor cell), macrophages, and NK cells in the miR-204-5p overexpressing tumors. On the other hand, the CD4⁺ T cells and CD8⁺ T cells including regulatory T cells showed significantly increased prevalence in the microenvironment of the miR-204-5p overexpressing tumors. We also characterized the immune cell composition of the paired spleen of the syngeneic mouse models and observed a significant reduction in myeloid cell population including MDSCs (Fig. 7K; Supplementary Fig. S10E and S10F). Taken together, our data suggest that miR-204-5p can be a key regulator of the tumor immune microenvironment by mobilizing different types of the myeloid and T cells in addition to its role in controlling cancer cell autonomous behaviors such as proliferation and metastasis.

Discussion

Here, we performed a genome-wide approach to discover deregulated miRNAs in breast cancer tissues versus adjacent normal tissues, and identified a substantial number of differentially expressed miRNAs including miR-204-5p. By overexpressing miR-204-5p in triple negative breast cancer cell lines, we show that miR-204-5p expression was significantly associated with various *in vitro* cell behaviors such as proliferation, migration, and metabolic properties. Furthermore, the mouse xenograft models and metastasis models showed that miR-204-5p critically regulates the process of breast cancer growth and metastasis *in vivo*. The levels of miR-204-5p in human breast cancer tissues were significantly associated with prognosis and tumor characteristics.

Many studies have previously suggested that decreased expression of miR-204-5p is linked to tumorigenesis in various human tumors by controlling cell growth, apoptosis, epithelial-mesenchymal transition, angiogenesis and chemotherapeutic sensitivity (6-9, 27-29). Li et al (13) have demonstrated that miR-204 was down-regulated in breast cancer and its expression had prognostic importance. However, in other reports, miR-204-5p was shown to exert a pro-proliferative effect in breast cancer cells and prostate cancer cells suggesting possible dual regulatory roles of miR-204-5p (10, 12). In the present study, we observed that there is a non-monotonic association between miR-204-5p expression and survival outcome of breast cancer patients. Furthermore, using a series of stable clones which ectopically overexpress miR-204-5p to different levels, we provide evidences that miR-204-5p possesses biphasic dose responses on breast cancer cell growth and metastasis.

A non-linear or biphasic dose response is commonly observed in various biological processes including gene expression regulations (30). Several studies have also suggested that the efficacy of target inhibition by miRNAs often show non-linear characteristics which make miRNA the fine-tuners of gene expression (31-35). For examples, miR-17-92 cluster affected cell viability in a dose-dependent and nonlinear fashion due to the dose-dependent target selection (32). The regulation of glioma cell proliferation and invasion by miR-9 is biphasic (34), and miR-96 can promote or inhibit autophagy by inhibiting its target genes depending on its expression levels (35). Here, by using the syngeneic 4T1 murine allograft breast cancer model, we show that the ability to grow tumor and to metastasize differs significantly among the various miR-204-5p overexpressing clone that carries

different levels of expression. Along with our observation of differential prognostic implication of miR-204-5p in TCGA dataset, our data provides evidence that the biological role of miR-204-5p may depend on the optimal saturation levels which can explain the inconsistent reports on the role of miR-204-5p in the previous reports (36). However, further studies are required to understand the complex roles of miR-204-5p in breast cancer progression, along with its target genes selectivity or binding affinity based on the expression level.

Our study also demonstrates that miR-204-5p significantly influence various cancer-related signaling pathways of breast cancer including PI3K/Akt pathway especially in basal subtype. Our results are in consistent with the previous studies showing the association between miR-204-5p and PI3K/Akt/Rac1 signaling or STAT3/BCI-2/survivin pathway in cancer cell lines (14, 27). Furthermore, we show evidence that miR-204-5p directly regulates the expression of PIK3CB which is an important regulator of the PI3K signaling activity (37, 38). Crowder et al (39) have shown that PIK3CB is highly expressed in luminal B subtype breast cancer tissues and carries important survival role in ER positive breast cancer cells. Our study demonstrates that PIK3CB is an important regulator of miR-204-5p-dependent PI3K/Akt signaling activity in basal breast cancer as well.

Our study also provides interesting observation that the miR-204-5p can alter the nature of immune microenvironment in breast cancer. Our data show that miR-204-5p expression was significantly associated with regulation of genes involved in TNF signaling pathway and cytokine-related pathway. Overexpression of miR-204-5p resulted in down-regulation of immune-related cytokines and resulted in a significant shift in microenvironmental immune cell compositions including reduction in MDSC, macrophage, and NK cells. Recent studies have revealed the complex interactions between the cancer cells and the surrounding immune microenvironment (40), and miRNA can contribute a critical regulatory role in shaping immune and inflammatory microenvironments in solid tumors (41). The reduction of myeloid cells in miR-204-5p-expressing tumor microenvironment may explain the metastasis-suppressing effect of miR-204-5p since myeloid cells in primary tumor and peripheral lymphoid organs not only promote metastasis process but can also orchestrate the development of pre-metastatic niche (42, 43). The potential roles for miR-204-5p during the dynamic process of tumor-microenvironment interactions that warrant further researches.

Also, the possibility of immune-modulating effect of miR-204-5p via PI3K signaling should be explored since PI3K pathways can influence the dynamic tumor-stroma interactions including angiogenesis and inflammation in solid tumors (44, 45).

Our study has several important limitations. First of all, our *in vitro* and *in vivo* studies have focused on the role of miR-204-5p in basal breast cancer cells. Although the TCGA dataset show highest correlation between miR-204-5p and downstream PI3K signaling pathways in basal subtype of breast cancer, it is still possible that miR-204-5p plays pivotal roles in other molecular subtypes considering similar degree of differential expression of miR-204-5p in tumor and normal tissues. Future studies investigating the roles of miR-204-5p are needed in other breast cancer subtypes with distinctly different biology. Second, despite the biochemical evidence of miR-204-5p targeting PI3KCB, we cannot exclude other key genes that may contribute to the tumor-suppressive role of miR-204-5p. It is possible that miR-204-5p has complex regulatory effect on diverse genes since silencing PIK3CB resulted in less phenotype changes when compared to that of miR-204-5p. While the PIK3CB overexpression showed concordant results in control cells, the PIK3CB rescue did not induce significant increase in PIK3CB protein levels in miR-204-5p overexpressing cells which might be due to the inhibitory effect of the miRNA. Another limitation is that our analysis on the mouse microenvironment mRNA profiles in MDA-MB-231 xenograft tumors might not fully represent the human microenvironment since we used severely immunocompromised mice. Lastly, we could not describe more comprehensive profiling of tumor microenvironment related to the different levels of miR-204-5p. Further characterization of immune microenvironment in response to miR-204-5p including characterization of diverse immune cell infiltration is needed to obtain more clear roles of miR-204-5p in breast cancer progression.

In conclusion, our results show that the miR-204-5p, which is a highly down-regulated gene in breast cancer tissue, is a tumor suppressor miRNA and regulates the process of tumor growth and metastasis in breast cancer. MiR-204-5p directly controls the expression of PIK3CB and downstream PI3K/Akt signaling activities, and the expression levels of miR-204-5p and PIK3CB are significantly associated with treatment outcome and pathologic features of human breast cancer. Additionally, the immune microenvironment of the allograft tumors showed substantial degrees of reprogramming in

miR-204-5p overexpressing tumors. Further understanding of the biologic role of miR-204-5p in breast cancer can provide novel insights of the complex process of breast cancer progression and metastasis.

Acknowledgements

This work was supported by the Basic Science Research Program through the National Research Foundation of Korea (NRF) funded by the Ministry of Education, Science and Technology (2015R1C1A1A02036629, 2015R1D1A1A02061904), by the grant from the National R&D Program for Cancer Control, Ministry for Health and Welfare, Republic of Korea (HA15C0011), and by the grant of the Korea Health Industry Development Institute (KHIDI), funded by the Ministry of Health & Welfare, Republic of Korea (HI13C2148), by the grant no 04-2016-0880 from SNUH Research Fund.

References

1. Calin GA, and Croce CM. MicroRNA signatures in human cancers. *Nat Rev Cancer*. 2006;6(11):857-66.
2. Croce CM. Causes and consequences of microRNA dysregulation in cancer. *Nat Rev Genet*. 2009;10(10):704-14.
3. Iorio MV, Ferracin M, Liu CG, Veronese A, Spizzo R, Sabbioni S, et al. MicroRNA gene expression deregulation in human breast cancer. *Cancer Res*. 2005;65(16):7065-70.
4. Kurozumi S, Yamaguchi Y, Kurosumi M, Ohira M, Matsumoto H, and Horiguchi J. Recent trends in microRNA research into breast cancer with particular focus on the associations between microRNAs and intrinsic subtypes. *J Hum Genet*. 2017;62(1):15-24.
5. Blenkinson C, Goldstein LD, Thorne NP, Spiteri I, Chin SF, Dunning MJ, et al. MicroRNA expression profiling of human breast cancer identifies new markers of tumor subtype. *Genome Biol*. 2007;8(10):R214.
6. Yin Y, Zhang B, Wang W, Fei B, Quan C, Zhang J, et al. miR-204-5p inhibits proliferation and invasion and enhances chemotherapeutic sensitivity of colorectal cancer cells by downregulating RAB22A. *Clin Cancer Res*. 2014;20(23):6187-99.
7. Bao W, Wang HH, Tian FJ, He XY, Qiu MT, Wang JY, et al. A TrkB-STAT3-miR-204-5p regulatory circuitry controls proliferation and invasion of endometrial carcinoma cells. *Mol Cancer*. 2013;12:155.
8. Xia Z, Liu F, Zhang J, and Liu L. Decreased Expression of MiRNA-204-5p Contributes to Glioma Progression and Promotes Glioma Cell Growth, Migration and Invasion. *PLoS One*. 2015;10(7):e0132399.
9. Liu L, Wang J, Li X, Ma J, Shi C, Zhu H, et al. MiR-204-5p suppresses cell proliferation by inhibiting IGFBP5 in papillary thyroid carcinoma. *Biochem Biophys Res Commun*. 2015;457(4):621-6.
10. Li T, Pan H, and Li R. The dual regulatory role of miR-204 in cancer. *Tumour Biol*. 2016;37(9):11667-77.
11. Findlay VJ, Turner DP, Moussa O, and Watson DK. MicroRNA-mediated inhibition of prostate-derived Ets factor messenger RNA translation affects prostate-derived Ets factor regulatory networks in human breast cancer. *Cancer Res*. 2008;68(20):8499-506.
12. Lee H, Lee S, Bae H, Kang HS, and Kim SJ. Genome-wide identification of target genes for miR-204 and miR-211 identifies their proliferation stimulatory role in breast cancer cells. *Sci Rep*. 2016;6:25287.
13. Li W, Jin X, Zhang Q, Zhang G, Deng X, and Ma L. Decreased expression of miR-204 is associated with poor prognosis in patients with breast cancer. *Int J Clin Exp Pathol*. 2014;7(6):3287-92.
14. Imam JS, Plyler JR, Bansal H, Prajapati S, Bansal S, Rebeles J, et al. Genomic loss of tumor suppressor miRNA-204 promotes cancer cell migration and invasion by activating AKT/mTOR/Rac1 signaling and actin reorganization. *PLoS One*. 2012;7(12):e52397.
15. Chung YR, Kim H, Park SY, Park IA, Jang JJ, Choe JY, et al. Distinctive role of SIRT1 expression on tumor invasion and metastasis in breast cancer by molecular subtype. *Hum Pathol*. 2015;46(7):1027-35.
16. McMillan KS, McCluskey AG, Sorensen A, Boyd M, and Zagnoni M. Emulsion technologies for

- multicellular tumour spheroid radiation assays. *Analyst*. 2016;141(1):100-10.
17. Tuominen VJ, Ruotoistenmaki S, Viitanen A, Jumppanen M, and Isola J. ImmunoRatio: a publicly available web application for quantitative image analysis of estrogen receptor (ER), progesterone receptor (PR), and Ki-67. *Breast Cancer Res*. 2010;12(4):R56.
 18. Jin Y, Chen Z, Liu X, and Zhou X. Evaluating the microRNA targeting sites by luciferase reporter gene assay. *Methods Mol Biol*. 2013;936:117-27.
 19. Kim D, Lee H, Koh J, Ko JS, Yoon BR, Jeon YK, et al. Cytosolic Pellino-1-Mediated K63-Linked Ubiquitination of IRF5 in M1 Macrophages Regulates Glucose Intolerance in Obesity. *Cell Rep*. 2017;20(4):832-45.
 20. Hall DP, Cost NG, Hegde S, Kellner E, Mikhaylova O, Stratton Y, et al. TRPM3 and miR-204 establish a regulatory circuit that controls oncogenic autophagy in clear cell renal cell carcinoma. *Cancer Cell*. 2014;26(5):738-53.
 21. Totaro A, Panciera T, and Piccolo S. YAP/TAZ upstream signals and downstream responses. *Nat Cell Biol*. 2018;20(8):888-99.
 22. Ardestani A, Lupse B, and Maedler K. Hippo Signaling: Key Emerging Pathway in Cellular and Whole-Body Metabolism. *Trends Endocrinol Metab*. 2018;29(7):492-509.
 23. Zhang Y, Kwok-Shing Ng P, Kucherlapati M, Chen F, Liu Y, Tsang YH, et al. A Pan-Cancer Proteogenomic Atlas of PI3K/AKT/mTOR Pathway Alterations. *Cancer Cell*. 2017;31(6):820-32 e3.
 24. West KA, Castillo SS, and Dennis PA. Activation of the PI3K/Akt pathway and chemotherapeutic resistance. *Drug Resist Updat*. 2002;5(6):234-48.
 25. Kumar A, Redondo-Munoz J, Perez-Garcia V, Cortes I, Chagoyen M, and Carrera AC. Nuclear but not cytosolic phosphoinositide 3-kinase beta has an essential function in cell survival. *Mol Cell Biol*. 2011;31(10):2122-33.
 26. DuPre SA, and Hunter KW, Jr. Murine mammary carcinoma 4T1 induces a leukemoid reaction with splenomegaly: association with tumor-derived growth factors. *Exp Mol Pathol*. 2007;82(1):12-24.
 27. Wang X, Qiu W, Zhang G, Xu S, Gao Q, and Yang Z. MicroRNA-204 targets JAK2 in breast cancer and induces cell apoptosis through the STAT3/BCI-2/survivin pathway. *Int J Clin Exp Pathol*. 2015;8(5):5017-25.
 28. Zeng J, Wei M, Shi R, Cai C, Liu X, Li T, et al. MiR-204-5p/Six1 feedback loop promotes epithelial-mesenchymal transition in breast cancer. *Tumour Biol*. 2016;37(2):2729-35.
 29. Flores-Perez A, Marchat LA, Rodriguez-Cuevas S, Bautista-Pina V, Hidalgo-Miranda A, Ocampo EA, et al. Dual targeting of ANGPT1 and TGFBR2 genes by miR-204 controls angiogenesis in breast cancer. *Sci Rep*. 2016;6:34504.
 30. Kim J, Choi M, Kim JR, Jin H, Kim VN, and Cho KH. The co-regulation mechanism of transcription factors in the human gene regulatory network. *Nucleic Acids Res*. 2012;40(18):8849-61.
 31. Ebert MS, and Sharp PA. Roles for microRNAs in conferring robustness to biological processes. *Cell*. 2012;149(3):515-24.
 32. Shu J, Xia Z, Li L, Liang ET, Slipek N, Shen D, et al. Dose-dependent differential mRNA target

- selection and regulation by let-7a-7f and miR-17-92 cluster microRNAs. *RNA Biol.* 2012;9(10):1275-87.
33. Jin HY, Oda H, Chen P, Yang C, Zhou X, Kang SG, et al. Differential Sensitivity of Target Genes to Translational Repression by miR-17~92. *PLoS Genet.* 2017;13(2):e1006623.
 34. Katakowski M, Charteris N, Chopp M, and Khain E. Density-Dependent Regulation of Glioma Cell Proliferation and Invasion Mediated by miR-9. *Cancer Microenviron.* 2016;9(2-3):149-59.
 35. Ma Y, Yang HZ, Dong BJ, Zou HB, Zhou Y, Kong XM, et al. Biphasic regulation of autophagy by miR-96 in prostate cancer cells under hypoxia. *Oncotarget.* 2014;5(19):9169-82.
 36. Lee T, Wang N, Houel S, Coutts K, Old W, and Ahn N. Dosage and temporal thresholds in microRNA proteomics. *Mol Cell Proteomics.* 2015;14(2):289-302.
 37. Pazarentzos E, Giannikopoulos P, Hrustanovic G, St John J, Olivas VR, Gubens MA, et al. Oncogenic activation of the PI3-kinase p110beta isoform via the tumor-derived PIK3Cbeta(D1067V) kinase domain mutation. *Oncogene.* 2016;35(9):1198-205.
 38. Jia S, Liu Z, Zhang S, Liu P, Zhang L, Lee SH, et al. Essential roles of PI(3)K-p110beta in cell growth, metabolism and tumorigenesis. *Nature.* 2008;454(7205):776-9.
 39. Crowder RJ, Phommaly C, Tao Y, Hoog J, Luo J, Perou CM, et al. PIK3CA and PIK3CB inhibition produce synthetic lethality when combined with estrogen deprivation in estrogen receptor-positive breast cancer. *Cancer Res.* 2009;69(9):3955-62.
 40. Gajewski TF, Schreiber H, and Fu YX. Innate and adaptive immune cells in the tumor microenvironment. *Nat Immunol.* 2013;14(10):1014-22.
 41. Kuninty PR, Schnittert J, Storm G, and Prakash J. MicroRNA Targeting to Modulate Tumor Microenvironment. *Front Oncol.* 2016;6:3.
 42. Kim S, Takahashi H, Lin WW, Descargues P, Grivennikov S, Kim Y, et al. Carcinoma-produced factors activate myeloid cells through TLR2 to stimulate metastasis. *Nature.* 2009;457(7225):102-6.
 43. Psaila B, and Lyden D. The metastatic niche: adapting the foreign soil. *Nat Rev Cancer.* 2009;9(4):285-93.
 44. Okkenhaug K, Graupera M, and Vanhaesebroeck B. Targeting PI3K in Cancer: Impact on Tumor Cells, Their Protective Stroma, Angiogenesis, and Immunotherapy. *Cancer discovery.* 2016;6(10):1090-105.
 45. Hirsch E, Ciruolo E, Franco I, Ghigo A, and Martini M. PI3K in cancer-stroma interactions: bad in seed and ugly in soil. *Oncogene.* 2014;33(24):3083-90.

Figure Legends

Figure 1.

MiR-204-5p in breast cancer tissues and clinical outcomes. **A**, A heatmap of small RNA-seq results of the differentially expressed miRNAs between primary breast tumors and paired normal mammary tissues from 17 patients (three Luminal A, seven Luminal B, two HER2, and five TNBC). [\log_2FC] ≥ 1.5 , FDR < 0.05 , $\log_2CPM > 0.05$. FC, fold change; FDR, false discovery rate; CPM, counts per million. **B**, MiR-204-5p levels from small RNA-seq. **C**, miR-204-5p levels by qPCR in 32 pairs of breast cancer patients. **D**, *In situ* hybridization of miR-204-5p in breast cancer tissues. Scale bars, 100 μm . **E**, MiR-204-5p levels in breast cancer subtypes from TCGA BRCA miR-seq data, RPM, reads per million. **F**, Correlation between TRPM3 mRNA and miR-204-5p in TCGA dataset, TRPM3, transient receptor potential melastatin-3; RSEM, RNA-seq by expectation maximization. **G**, Methylation levels of two CpG loci in TRPM3 gene. **H** and **I**, The subtype-specific methylation levels of cg20555506 (**H**) and cg21251785 loci (**I**). **J** and **K**, Kaplan-Meier curves with (**J**) median and quartiles (**K**) of miR-204-5p expression from TCGA BRCA miRNA-seq (n=889). *P* values are determined by log-rank test. **L**, GSEA of KEGG pathway upregulated in the third quartile group compared to the other quartiles. Error bars denote means \pm SD. **P* < 0.005 , ***P* < 0.001 , ****P* < 0.0001 .

Figure 2.

MiR-204-5p-induced phenotypes in breast cancer cells. **A and B**, MiR-204-5p overexpression and breast cancer cell growth measured by CellTiter-Glo assay (A) and 3D spheroid growth at day 10 (B). **C**, Representative microscopic images of spheroids at day 10 (upper) and viability assay using LIVE/DEAD[®] Viability/Cytotoxicity Kit (lower). **D**, Transwell cell migration results at 24hr. **E**, Control and miR-204-5p overexpressing MDA-MB-231 cells were injected into the fatpads of NSG mice (n=3 mice/group). **F**, Representative images of H&E and Ki67 staining of tumors. The proliferation index was measured from 6 different images at 200x. **G** and **H**, Metastatic nodules in lung and liver stained with Bouin's solution (**G**) and H&E staining (**H**). **I**, KEGG pathways analysis of DEGs ($[\log_2FC] \geq 1$, mean FPKM ≥ 1 , adjusted *p* < 0.05) of human RNA expression data extracted from MDA-MB-231 xenograft tumor RNA-seq. Red dotted-line indicates the *P* value < 0.05 . **J**, oxygen consumption rates

(OCR) measured by sequentially treating cells with oligomycin (1 μm), FCCP (0.5 μm), rotenone/antimycin A (1 μm). **K**, Extracellular acidification rates (ECAR) measured by adding glucose (10 mM), oligomycin (1 μm), and 2-DG (50 nM). Scale bars, 100 μm (**C** and **D**) and 50 μm (**F** and **H**). Error bars denote means \pm SD. * $P < 0.005$, ** $P < 0.001$, *** $P < 0.0001$.

Figure 3.

Biphasic effects of miR-204-5p on breast cancer cells. **A**, The levels of miR-204-5p on four stable clones and control 4T1 measured by qPCR. **B** and **C**, Cells (2×10^5) stably expressing miR-204-5p or the control were injected into bilateral mammary fatpad ($n=6$ mice/group), and tumor volumes (B) and weights (C) were measured. **D**, H&E and Ki67 staining of 4T1 tumors. **E**, Levels of miR-204-5p in tumor tissues obtained from control 4T1 and four stable clones. ($n=10\sim 12$ for control, C#2, and C#3, $n=6$ for C#1 and C#4). **F**, Correlation between tumor weight and miR-204-5p expression in C#4. **G** and **H**, Lung metastasis at two weeks after injecting cells (2×10^5) into tail vein ($n=8\sim 10$ mice/group, except $n=4$ for C#4). **I**, The relative growth rate of control and miR-204-5p overexpressing 4T1 clones. **J**, Cells under confocal microscopy after staining with CellTracker (green) and F-actin (red). **K**, Western blot of E-cadherin in 4T1 clones overexpressing miR-204-5p. Scale bars, 200 μm (**D**, **H**; middle panel), 50 μm (**H**; lower panel) and 100 μm (**J**). Error bars denote means \pm SD. * $P < 0.005$, ** $P < 0.001$, *** $P < 0.0001$.

Figure 4.

Regulation of PIK3CB by miR-204-5p. **A**, Pathways enrichments analysis of differentially expressed genes ($[FC] > 1.5$, $p < 0.05$) using KEGG database. **B** and **C**, Association of miR-204-5p and the degree of protein phosphorylation (B) or PI3K/Akt signature (C) in basal-like breast cancer ($n=89$). **D**, The putative miR-204-5p binding sites; the wild-type and mutant (Mut) sequence of 3'-UTR of Pik3cb (mmu-ST1 and mmu-ST2), PIK3CB (hsa-ST1). **E**, Luciferase assay in HEK293FT cells co-transfected with various reporter vector constructs (50 ng) with control or miR-204-5p mimics (50 nM). **F** and **G**, Expression level of PIK3CB mRNA in 4T1 and MDA-MB-231 overexpressing control and miR-204-5p. **H**, Western blot of PIK3CB and phosphor-Akt in 4T1 and MDA-MB-231 cells. **I**, Representative

images of PIK3CB staining of tumors derived from 4T1 and MDA-MB-231 and the percentage of PIK3CB positive cells. Scale bars, 50 μ m. Error bars denote means \pm SD. ** $P < 0.001$, *** $P < 0.0001$.

Figure 5.

Effects of PIK3CB on breast cancer cells. **A-B**, mRNA (A) and protein (B) level of PIK3CB after siPIK3CB treatment. **C-D**, On day 3 after transfection, cell proliferation was examined with CellTiter Glo (C) and 3D Matrigel assay (D). **E**, Transwell migration assay of transfected cells. **F**, Western blots of PIK3CB after PIK3CB overexpression in control and miR-204-5p-overexpressing MDA-MB-231 cells. **G-H**, Results of CellTiter Glo proliferation assay (G), and migration assay (H). **I**, Viability of control and miR-204-5p overexpressing MDA-MB-231 cells treated with TGX-221. **J**, Viability of cells treated with TGX-221 (10 μ M) or GSK2636661 (10 μ M) for 24 h. NTC, not treated control. **K**, Cell viability with doxorubicin (0.3 μ M), bortezomib (10 nM), paclitaxel, (100 nM) docetaxel (10 nM), and 5-FU (1 μ M) for 24 h. The relative growth rate or viability after drug treatment was measured by CellTiter Glo reagent (I-K). Error bars denote mean \pm SD. * $P < 0.001$. ** $P < 0.005$, *** $P < 0.0001$.

Figure 6.

PIK3CB in breast cancer tissues and cells. **A and B**, The mRNA levels of PIK3CB in breast cancer tissue in 17 cases including six paired normal tissues quantified by qPCR. L, Luminal; T, TNBC. **C**, PIK3CB levels in 112 paired TCGA cases. **D-G**, Expression and correlation analysis of miR-204-5p and PIK3CB from TCGA data. PIK3CB expression was compared based on miR-204-5p expression levels in all breast cancer cases (D and E) and in basal subtype cases (F and G). **H**, Breast cancer cell lines stained with CellTracker (green), PIK3CB (red), and DAPI (blue). **I**, Kaplan-Meier survival plot showing overall survival according to PIK3CB levels. **J**, Histologic images of PIK3CB expression pattern; negative, cytoplasmic, and nucleus PIK3CB positive TMA tissues. Scale bars, 50 μ m. Error bars denote means \pm SD. *** $P < 0.0001$.

Figure 7.

Immune microenvironment reprogramming by miR-204-5p. **A**, Spleen weights from BALB/c nude mice bearing MDA-MB-231 xenografts. **B** and **C**, Representative images of H&E and CD11b staining of spleens and the percentage of CD11b positive cells. **D** and **E**, Expression levels of CCL20, VEGF-A and CSF1 mRNA in 4T1 (**D**) and MDA-MB-231 (**E**) cells. **F**, Secreted CCL20 and VEGF-A levels in 4T1 cells. **G** and **H**, Immunohistochemical staining against CCL20 and CD11b in mouse 4T1 tumors (**G**) and in MDA-MB-231 tumors (**H**). **I**, Top 20 upregulated KEGG pathways using DEGs ($[\log_2FC] \geq 1$, mean FPKM ≥ 1 , adjusted $p < 0.05$) in mouse RNA expression data extracted from MDA-MB-231 xenograft tumor RNA-seq. **J** and **K**, Summary of FACS analyses of immune cell populations in tumors (**J**) and spleens (**K**) derived from control and miR-204-5p-overexpressing 4T1 (C#3). Results are shown as a percent of total CD45+ cells in tumors and total cell numbers in spleen. Scale bars, 500 μm (**B**; left panel) and 50 μm (**B**; right panel, **C**, and **G**). Error bars denote means \pm SD. * $P < 0.005$, ** $P < 0.001$, *** $P < 0.0001$.

Figure 1

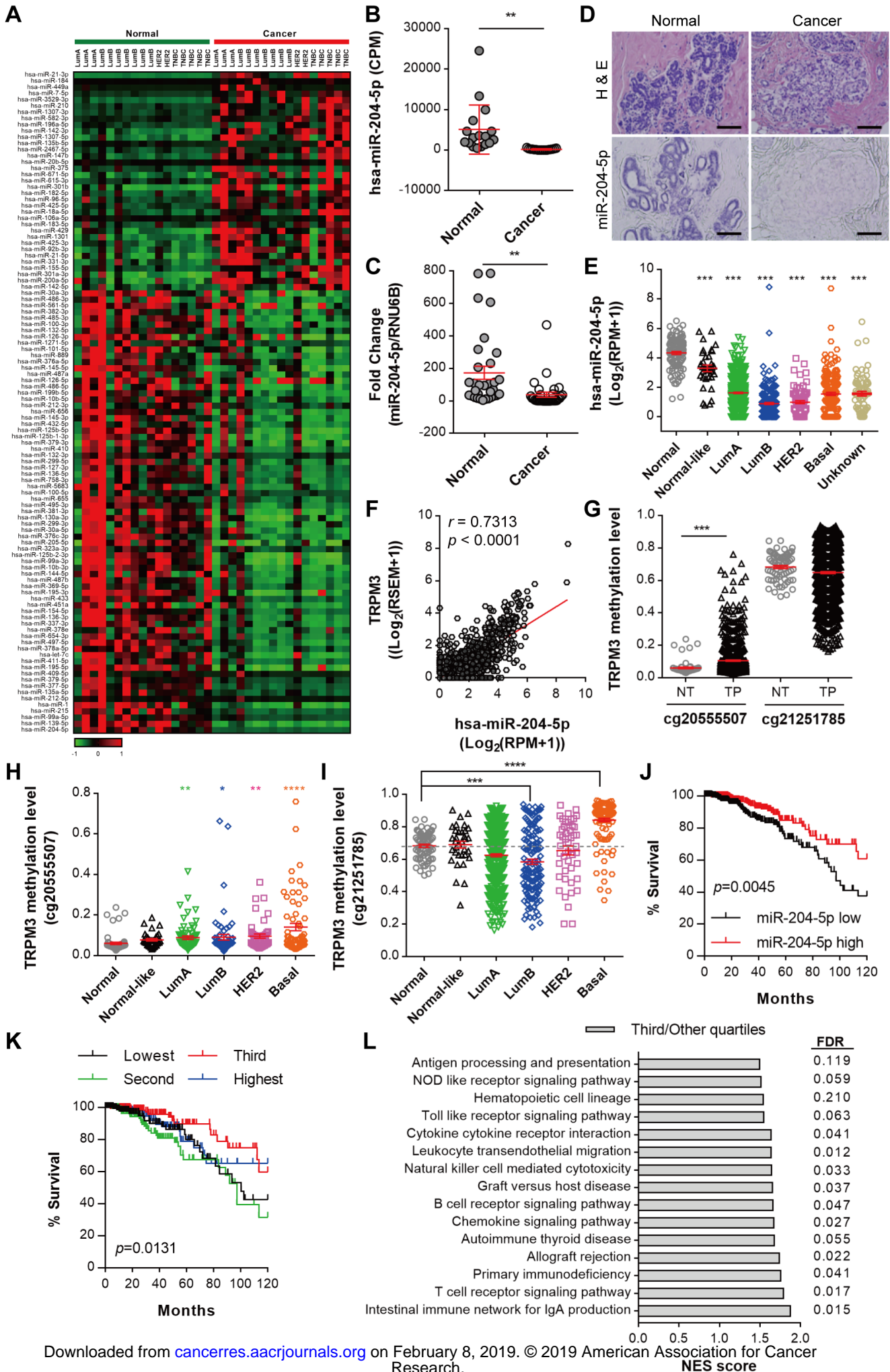


Figure 2

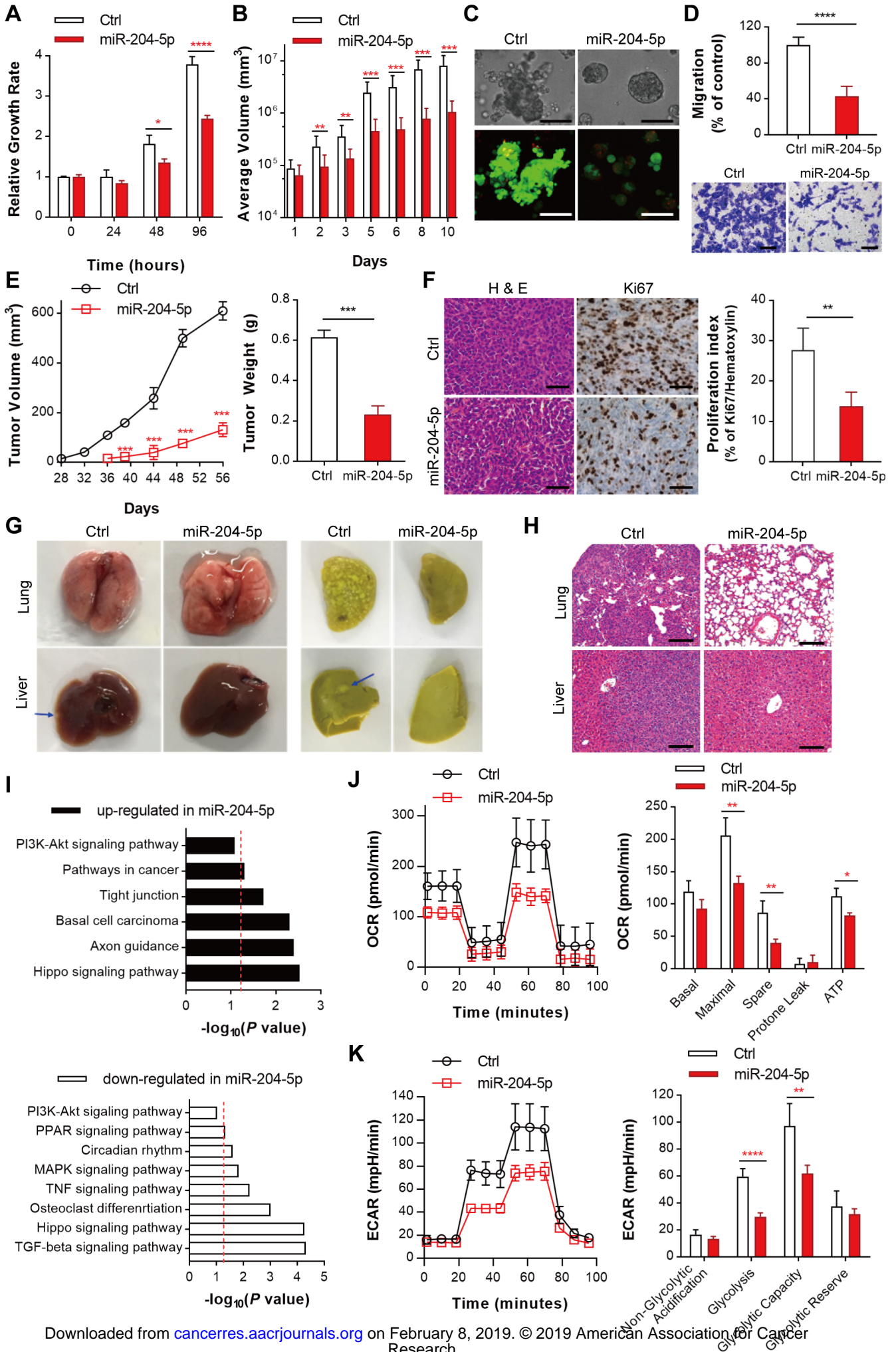


Figure 3

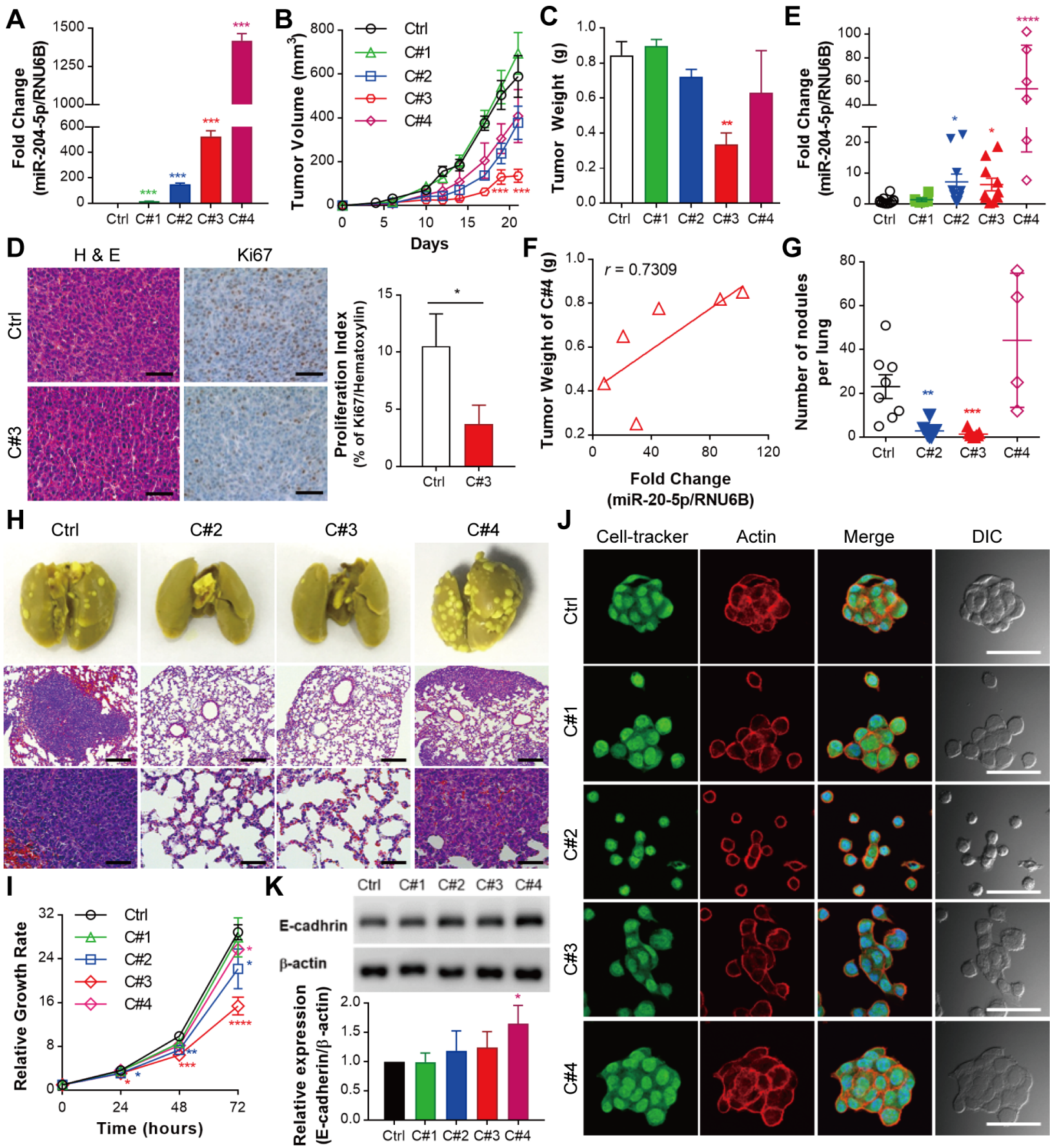
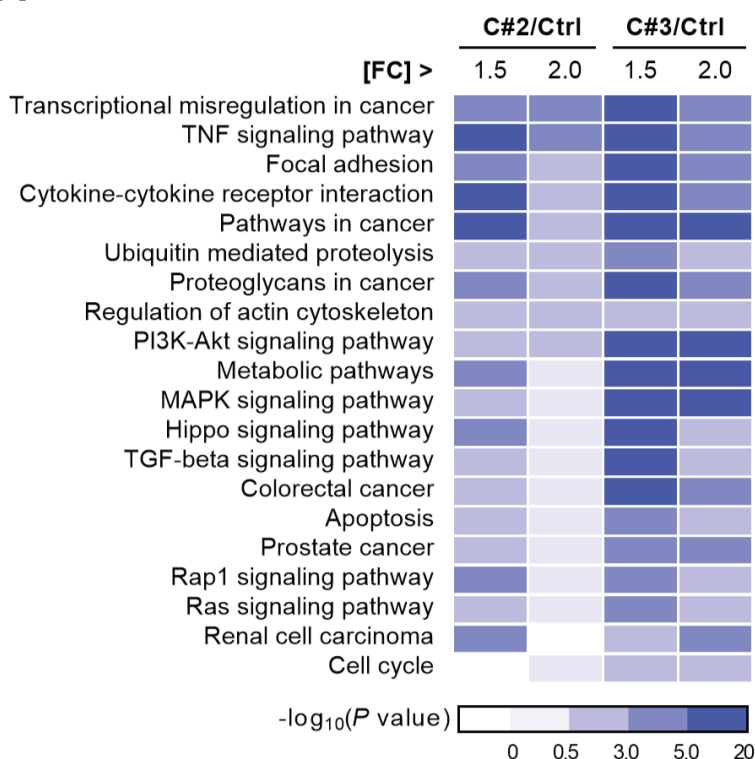
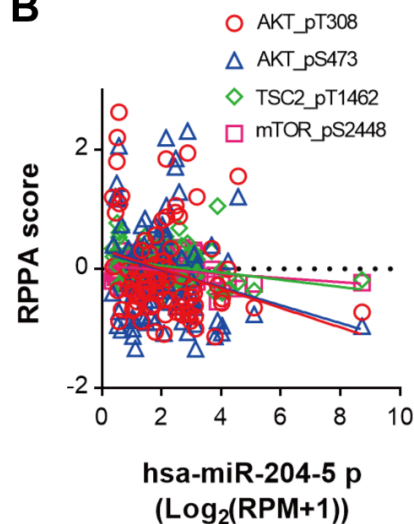


Figure 4

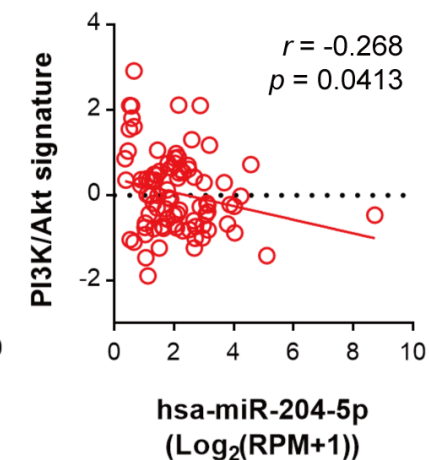
A



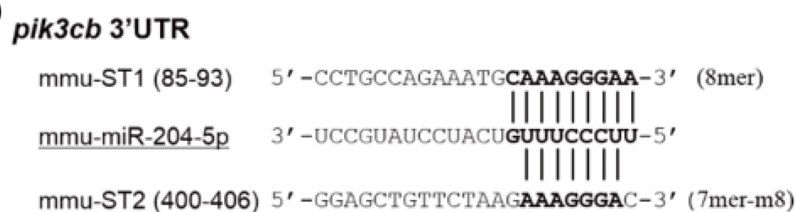
B



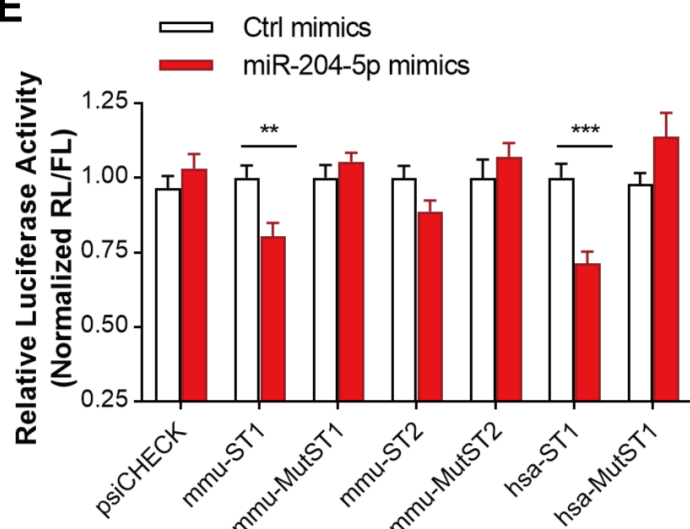
C



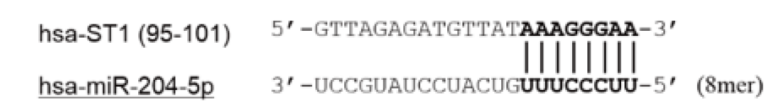
D



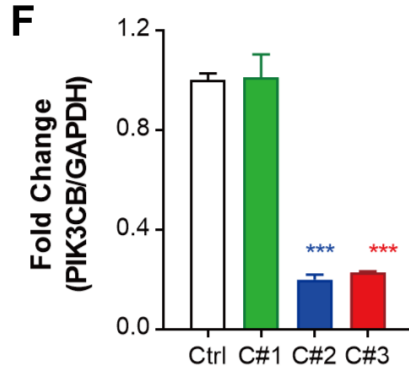
E



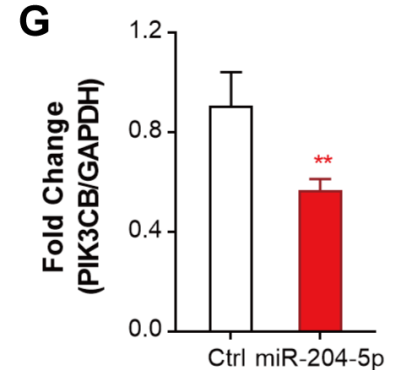
***PIK3CB* 3'UTR**



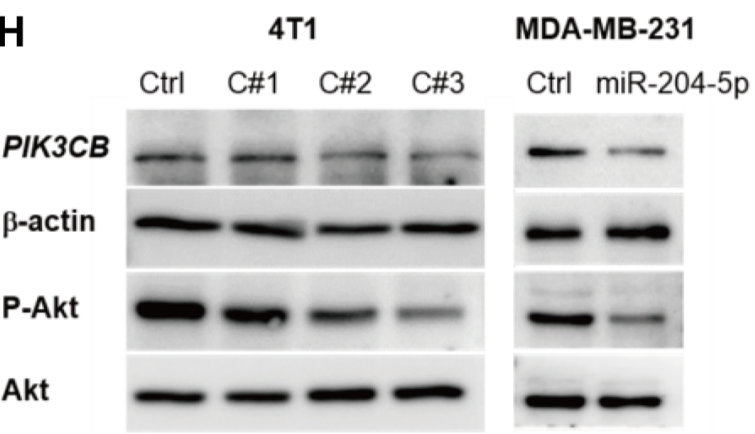
F



G



H



I

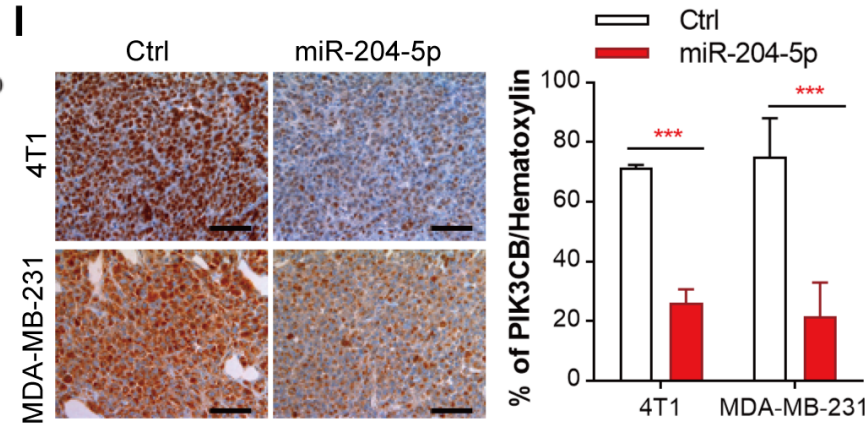


Figure 5

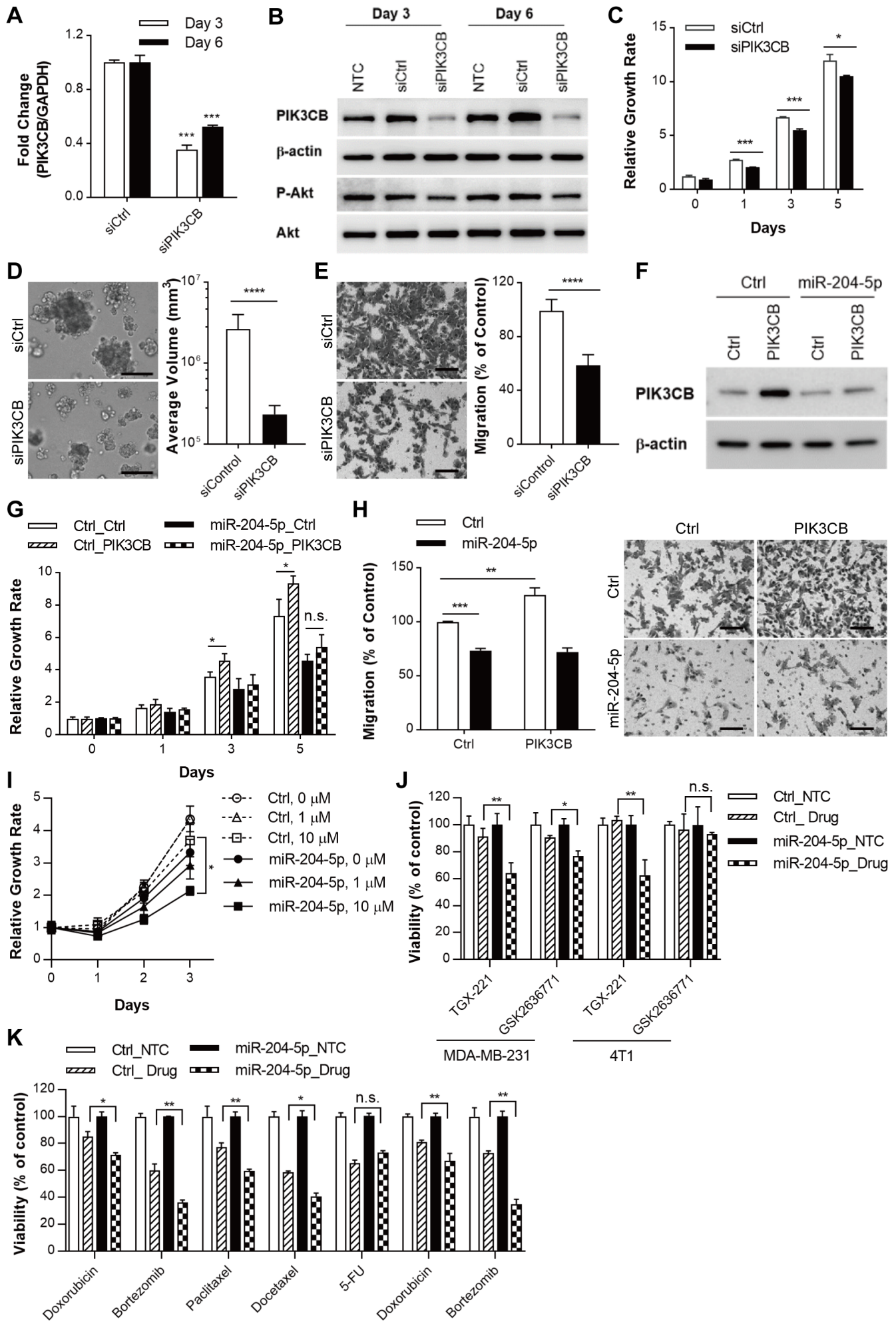


Figure 6

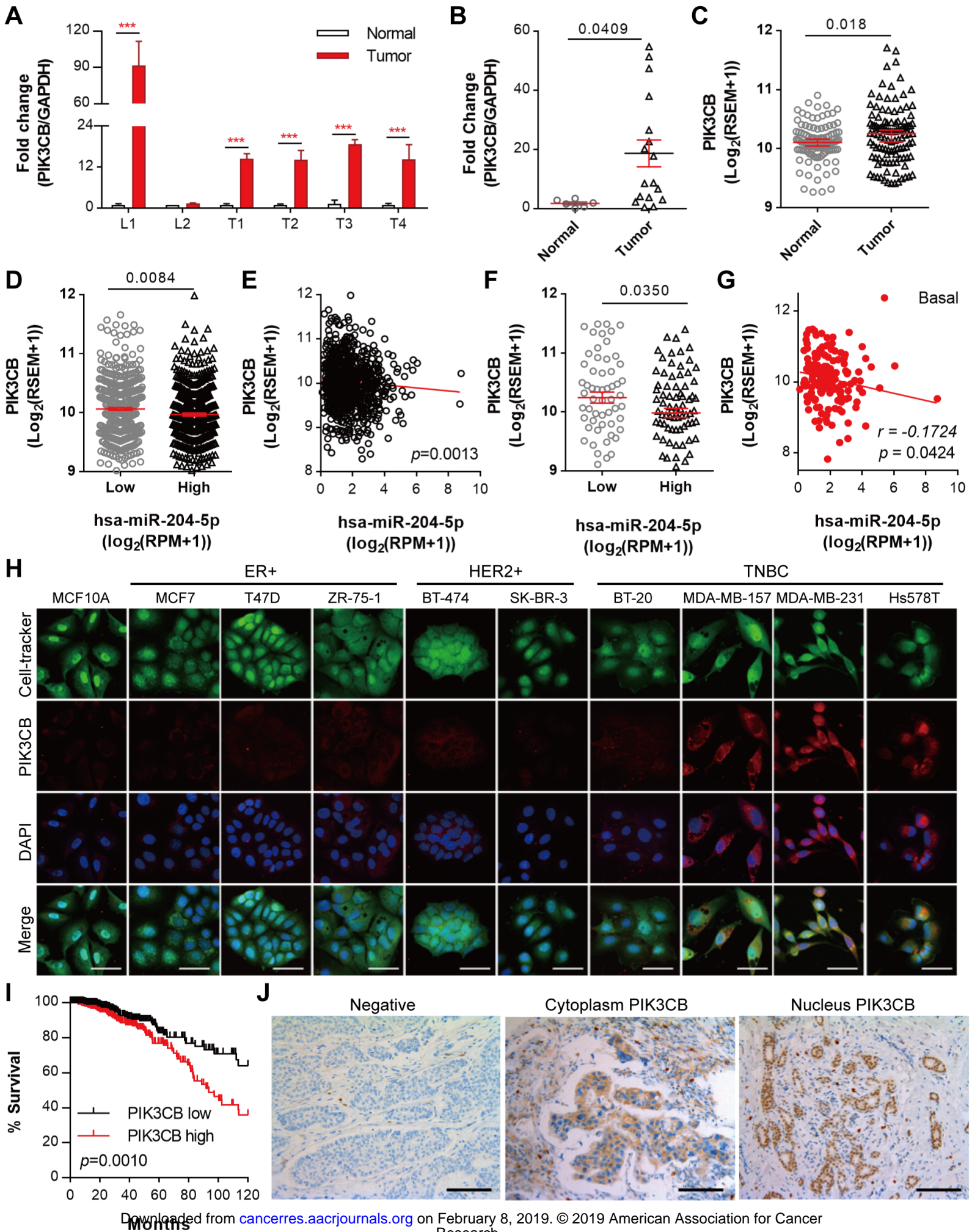
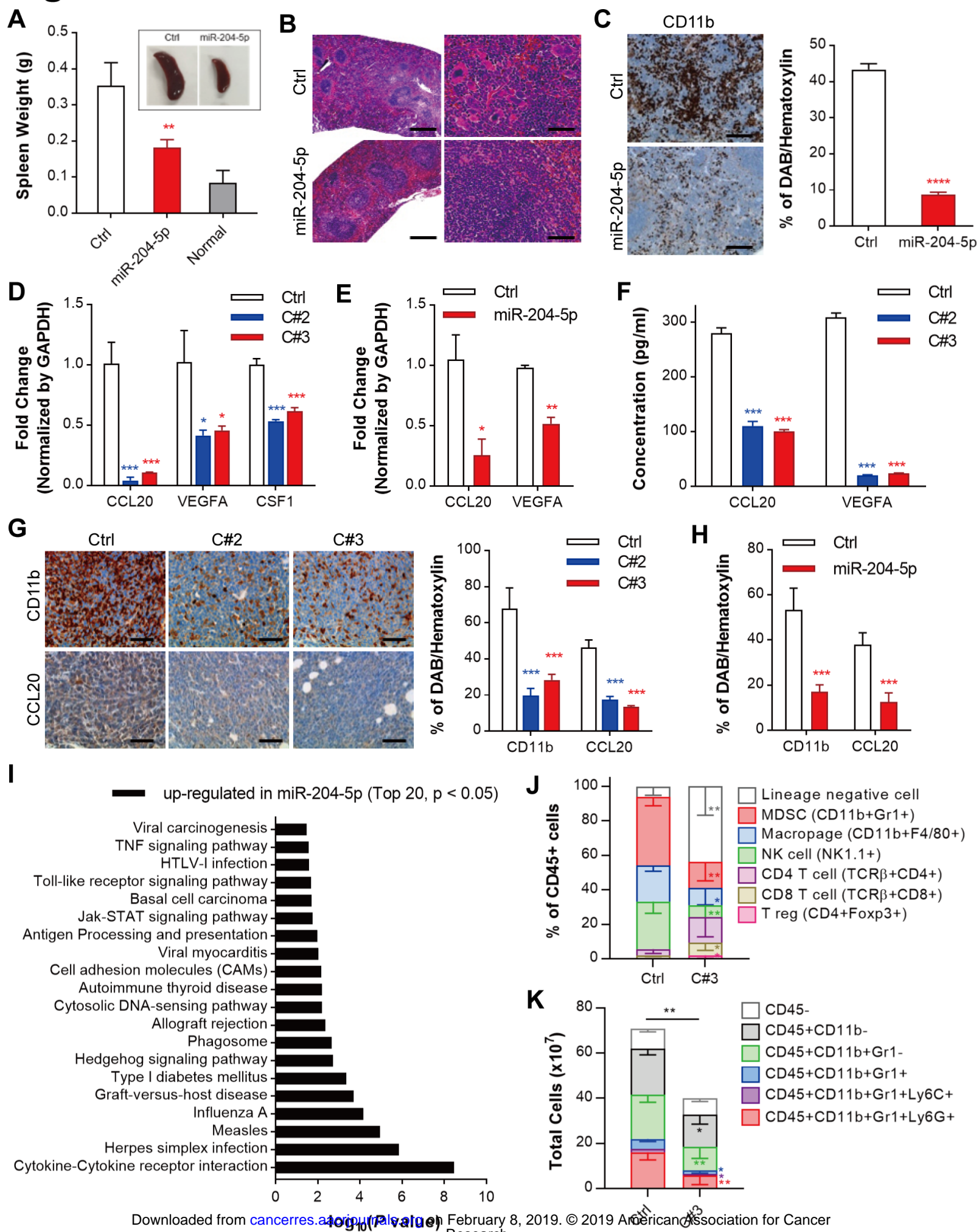


Figure 7



Cancer Research

The Journal of Cancer Research (1916–1930) | The American Journal of Cancer (1931–1940)

Tumor suppressor microRNA-204-5p regulates growth, metastasis, and immune microenvironment remodeling in breast cancer

Bok Sil Hong, Han Suk Ryu, Namshin Kim, et al.

Cancer Res Published OnlineFirst February 8, 2019.

Updated version	Access the most recent version of this article at: doi: 10.1158/0008-5472.CAN-18-0891
Supplementary Material	Access the most recent supplemental material at: http://cancerres.aacrjournals.org/content/suppl/2019/02/08/0008-5472.CAN-18-0891.DC1
Author Manuscript	Author manuscripts have been peer reviewed and accepted for publication but have not yet been edited.

E-mail alerts	Sign up to receive free email-alerts related to this article or journal.
Reprints and Subscriptions	To order reprints of this article or to subscribe to the journal, contact the AACR Publications Department at pubs@aacr.org .
Permissions	To request permission to re-use all or part of this article, use this link http://cancerres.aacrjournals.org/content/early/2019/02/08/0008-5472.CAN-18-0891 . Click on "Request Permissions" which will take you to the Copyright Clearance Center's (CCC) Rightslink site.